

Design and Development of Linear to Circular polarization convertor loaded Microstrip Antenna with Wide Impedance Bandwidth

Mukesh Tiwari¹, Kokab Afroz² and Mehajabeen Fatima³

^{1,2}Department of Electronics and Communication Engineering, Sri Satya Sai University of Technology & Medical Sciences, Sehore, Madhya Pradesh, India.

³Department of Electronics and Communication Engineering, Sagar Institute of Research & Technology, Bhopal, Madhya Pradesh, India.

ABSTRACT

In this communication, step by step process of linear to circular polarization (LP to CP) convertor loaded microstrip antenna is designed and investigated. The two main features of proposed antenna are: (i) the Q-factor of inset fed microstrip antenna become low by loading the pentagon shaped defected ground structure (DGS); and (ii) suspension of meta surface above the radiator converts the linear waves into circularly polarized waves. Experimental verification of proposed antenna confirms that the proposed antenna operates from 12.34 GHz-14.4 GHz. 3-dB axial ratio bandwidth is around 13.5 GHz to 14.25 GHz. Stable and broadside radiation pattern provides the antenna gain around 5.0dBi in the operating band. All these features make the designed radiator suitable for Ku Band Satellite Applications.

Keywords: Microstrip Antenna, Circular polarization, Defected Ground Structure

I. INTRODUCTION

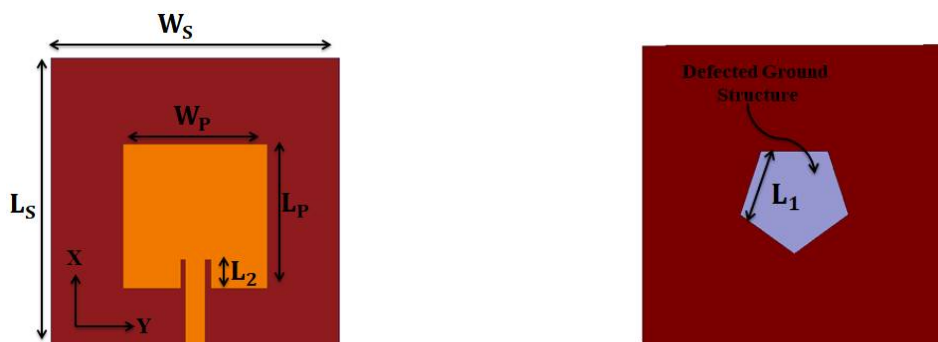
In the current wireless communication world, the main focus of antenna researchers is on the designing of circularly polarized antennas because of its several advantages such as making transmitter and receiver antenna orientation independent, reduce the effect of fading [1]. The integration of circular polarization feature with Microstrip antenna is one of the quite obvious choices for wireless communication system designers. It is due to its lots of advantages like compactness, low profile, conformal to planner/non planner surfaces [2].

In case of microstrip antenna, features of circular polarization are achieved by single feed [3] or by multi feed structure [4]. In case of single feed microstrip antenna design, achieved AR bandwidth is less, while the complexity is high in case of multi feed antenna design. Zhu et.al.proposed a suspended periodic structure over microstrip antenna for converting linear waves into circular wave. It gives the CP waves from 2.38 GHz-2.55 GHz [5].Paiva et.al.proposed tilted hexagonal ring shaped unit cell based metasurface for converting linear waves into circular. This metasurface is suspended over the microstrip antenna for getting CP waves from 2.36-2.49 GHz [6]. Similarly, metasurface is also used as LP to CP convertor in case of microstrip line fed slot antenna. It provides the CP bandwidth from 5.0 to 5.61 GHz [7]. Dong et.al.proposed a parasitic square cross gap based metasurface to convert linear waves obtained from slot antenna into circular waves. 3-dB ARBW achieved in this antenna is from 5.18 GHz to 6.19 GHz [8].

In the proposed antenna design, a meatsurface is used to convert the LP waves into CP waves created from inset fed microstrip antenna. The proposed antenna supports Ku band applications i.e. 12.34 GHz-14.36 GHz. DGS is used to improve the impedance bandwidth of proposed antenna. Wide CP bandwidth is also achieved from 12.9 GHz to 14.1 GHz. For good understanding of proposed antenna design, the article is divided in different sections: (i) antenna design layout, (ii) antenna analysis; (iii) experimental results; and (iv) conclusion.

II. Antenna Geometrical Layout

Structural layout of designed antenna is displayed in Fig.1. Inset microstrip line fed rectangular patch behave as a radiator. The proposed radiator along with metasurface (LP to CP convertor) is designed on FR4 substrate ($\epsilon_r = 4.4$ and $\tan \delta = 0.02$) having thickness 1.6 mm. Pentagon shaped slot has been etched from ground for making defected ground structure. Metasurface is suspended at a height (H_2) of 7.0 mm from the surface of the radiator. Table-1 lists the optimized antenna parameters of proposed antenna.



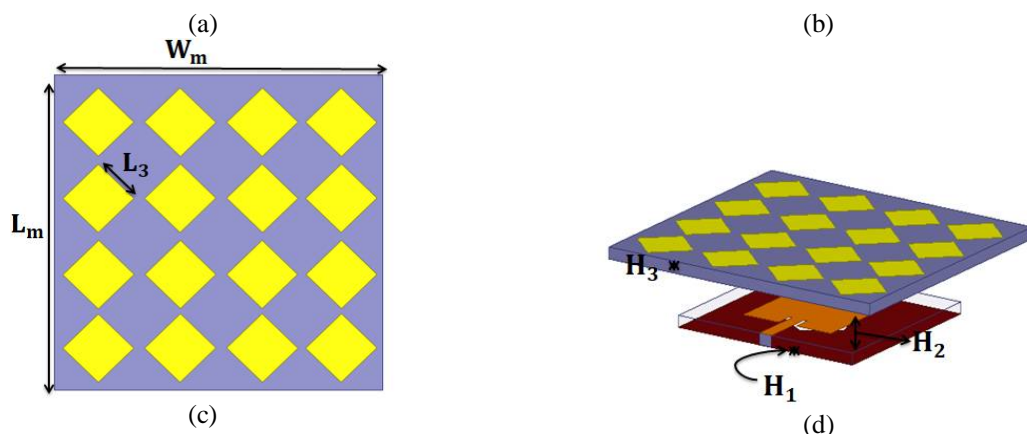


Fig. 1 Geometrical Layout of Proposed radiator (a) upper view of patch antenna (b) DGS loaded ground plane (c) proposed LP to CP converter (d) 3D view of proposed antenna

Table-1 Optimized values of different antenna parameters

Symbol	Dimension (mm)	Symbol	Dimension (mm)
L_S	40.0	W_P	20.0
W_S	40.0	L_P	20.0
L_M	60.0	L_1	10.0
H_3	1.6	L_2	4.0
H_1	1.6	L_3	9.25
W_M	60.0	H_2	7.0

III. Antenna Analysis

In this section, antenna analysis has been carried out using Ansys HFSS EM simulation software. Fig. 2 shows the different steps involved in designing of proposed antenna. Step-1 and step-2 indicates simple microstrip line and inset fed patch antenna respectively. Step-3 is simply pentagon shaped DGS loaded patch antenna. Step-4 is the proposed antenna design i.e. metasurface loaded patch antenna. Fig. 3 and Fig. 4 show the reflection coefficient and axial ratio variation for different steps involved shown in Fig.2. It is perceived from Fig. 3 that two resonant peaks are created due to simple microstrip patch at 12.2 GHz and 13.0 GHz. Inset feed improves the impedance matching of the resonant peak [9]. It also shifts the resonant peaks to 12.4 GHz and 13.4 GHz due to reduction in effective permittivity of radiator. Integration of defected ground structure reduces the Q-factor of patch antenna, which in turn improves the bandwidth. Loading of metasurface does not create a significant effect on the reflection coefficient of proposed radiator. From Fig. 4, it can be perceived that loading of metasurface over the patch radiator, converts the linearly polarized waves into circular polarization. It provides the circular polarization from 13.6 GHz to 14.2 GHz. Fig. 5 displays the magnitude distribution of E-field over the patch at 12.4 GHz and 13.4 GHz. From Fig. 5, it is observed that TM_{21} and TM_{22} mode is responsible for these resonant peaks [10].

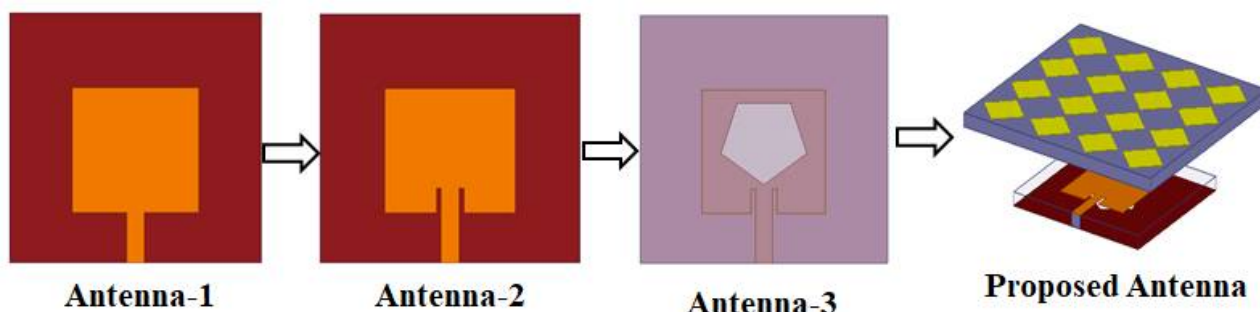


Fig. 2 Different Steps involved in designing of proposed antenna

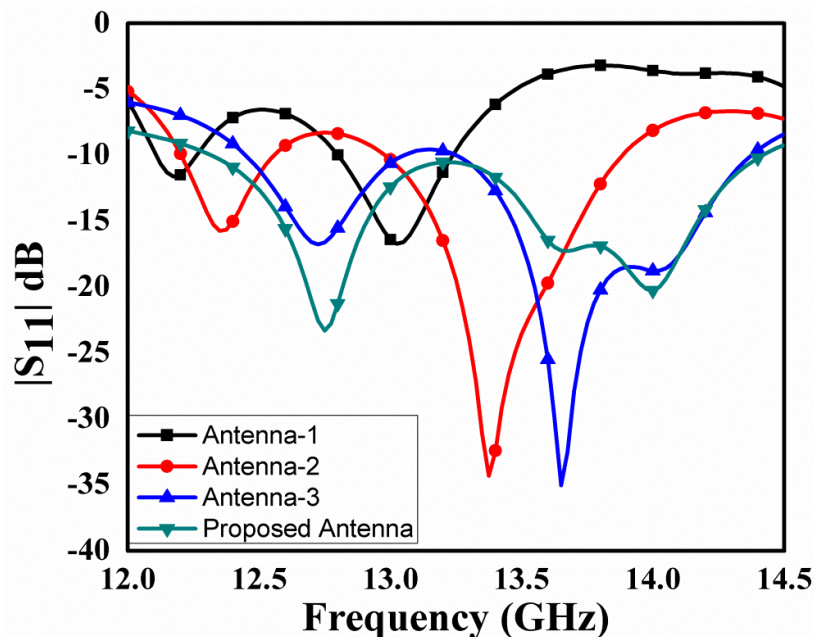


Fig. 3 |S₁₁| variation of different steps involved in proposed antenna

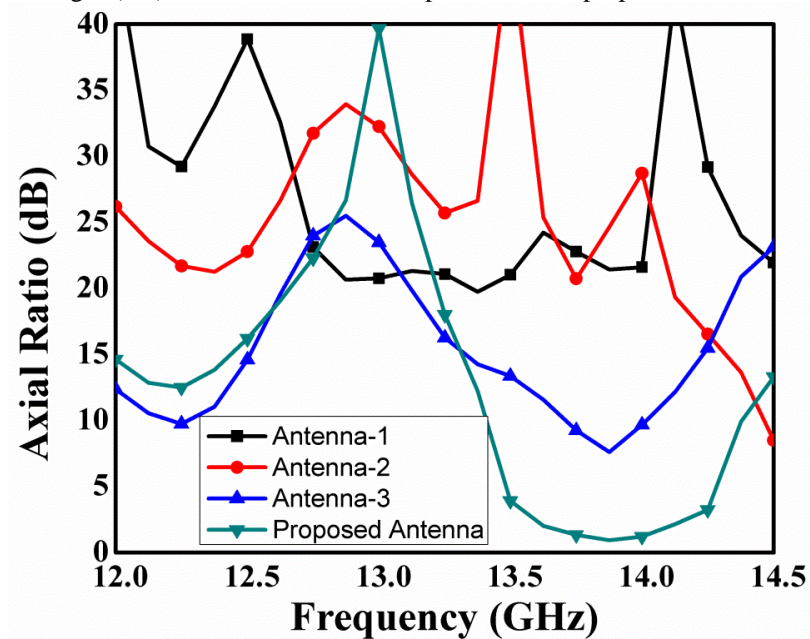


Fig. 4 Axial Ratio variation of different steps involved in proposed antenna

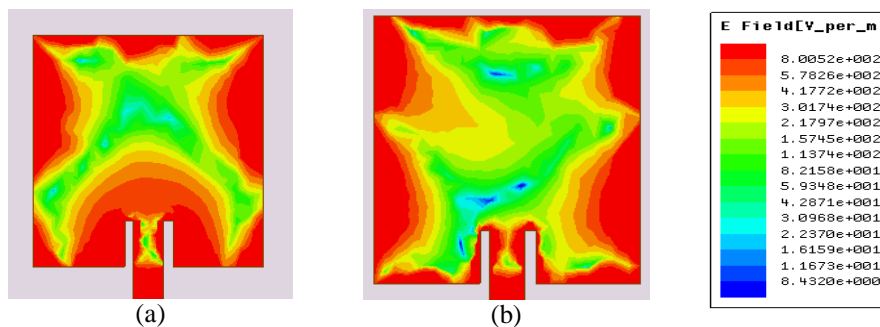


Fig. 5 E-field distribution on patch (a) 12.4 GHz (b) 13.4 GHz

Fig. 6 shows the variation of reflection coefficient with change in the dimension of pentagon shaped DGS. From Fig. 6, it can be observed that as the size of pentagon shaped DGS increases, there is improvement in the impedance bandwidth of antenna. It is due to the reduction in the capacitive effect of the antenna [11]. E-field alignment on the proposed metasurface is shown in Fig. 7. The upward and adjacent gaps of periodically organized rhombus shaped unit cell divide the waves into horizontal and vertical linear polarized waves with different phase angles i.e. 0° , 90° , 180° , 270° . Collectively, these waves provide the circular polarization. The main condition for CP wave generation is: degenerated orthogonal mode creation with equal amplitude and 90° shift between these orthogonal modes [12]. Fig. 8 shows the ratio of magnitude variation of two orthogonal modes as well as phase shift variation with in the operating range. It is clearly observed from Fig. 8 that ratio of two orthogonal modes is around 1.0 and phase shift is around 90° in between 13.6 GHz to 14.2 GHz. It is the condition of CP waves generation.

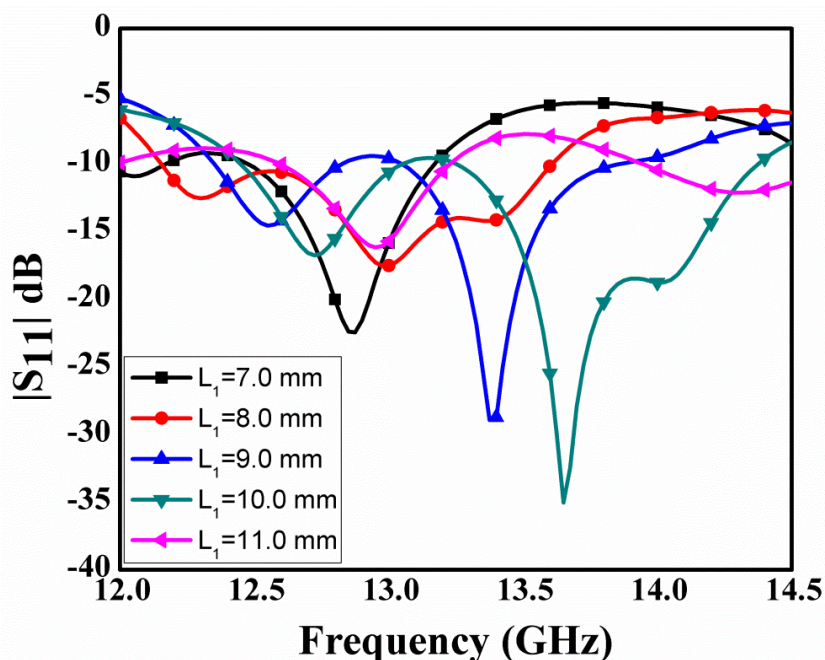


Fig. 6 Reflection Coefficient variation with change in length of the pentagon DGS

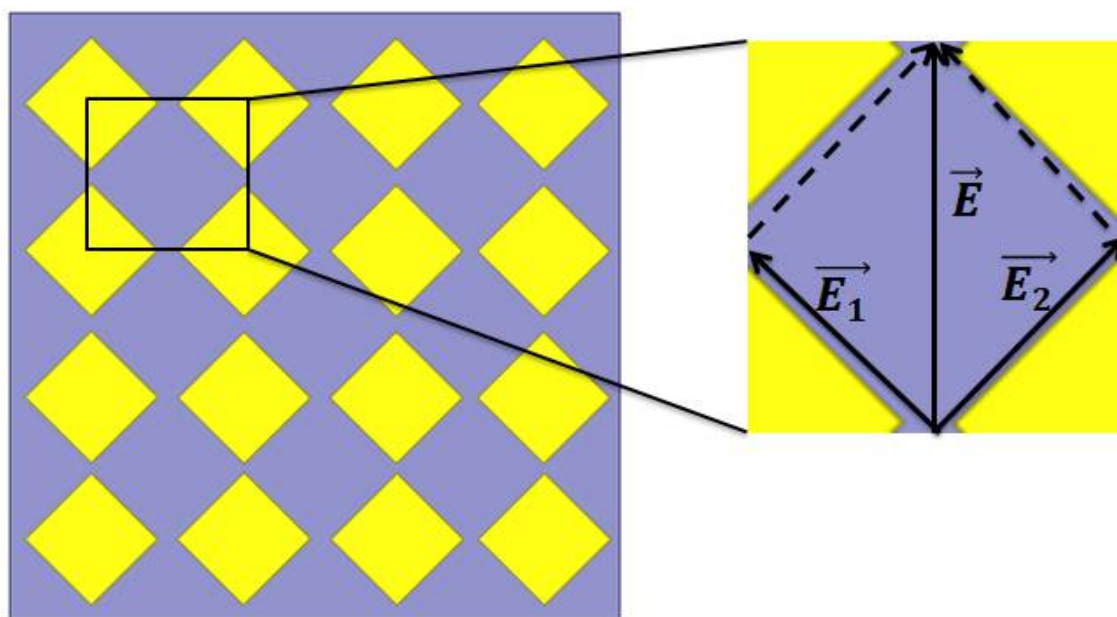


Fig. 7 E-field alignment on the proposed metasurface for LP to CP Converter

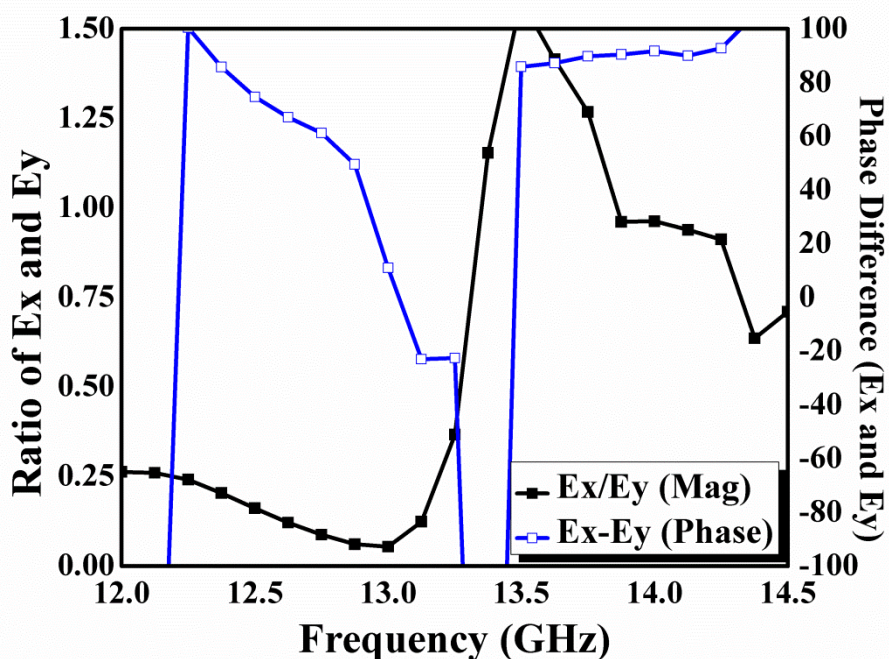


Fig. 8 Variation of ratio of magnitude and phase of orthogonal E-fields over the operating frequency range

Fig. 9 shows the axial ratio variation with change in the height (H_2) of metasurface with respect to radiator. From Fig. 9, it is confirmed that optimum value of 3-dB axial ratio bandwidth is obtained at 7.0 mm. Fig. 10 displays the axial ratio variation with change in the cell size i.e. L_3 . It is perceived from Fig. 10 that the optimum value of 3-dB AR bandwidth is achieved when $L_3 = 9.25$ mm.

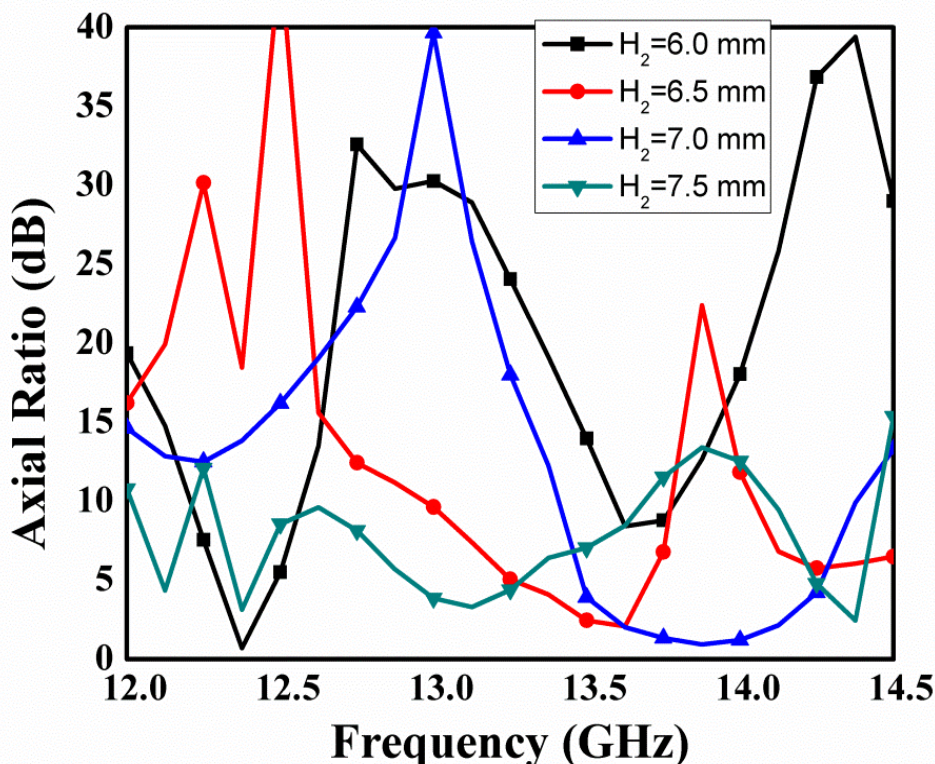


Fig. 9 Axial Ratio variation with change in height (H_2) of metasurface over the radiator

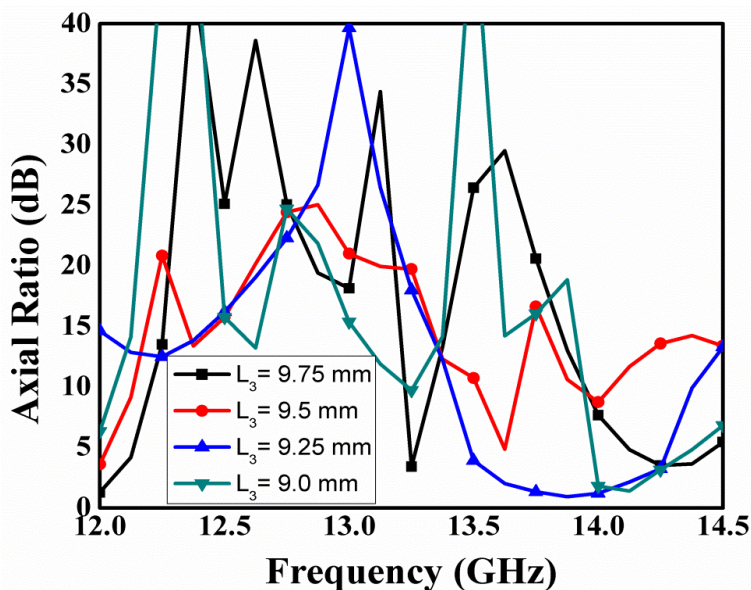


Fig. 10 Axial Ratio variation with change in the size of periodically arrange unit cell

IV. Experimental Outcome

In this section, experimental results are compared with simulated one for the verification purpose. Fabricated prototype is developed for the same and it is shown in Fig. 11. Its input parameter i.e. S_{11} is measured with the help of E8363C Keysight based PNA. Fig. 12 shows the comparison between measured and simulated $|S_{11}|$ of proposed antenna. From Fig. 12, it is confirmed that the proposed antenna works from 12.34 GHz-14.4 GHz. There is slight change in between measured and simulated $|S_{11}|$ due to different fabrication error such as difference in connector and substrate thickness. Fig. 13 shows the comparison between measured and simulated axial ratio variation. It is measured inside the anechoic chamber with the help of dual linear pattern measurement [12]. It is measured along the broadside direction. From Fig. 13, it can be said that there is good agreement between measured and simulated axial ratio. The proposed antenna design produces the CP waves in between 13.5 GHz to 14.25 GHz.

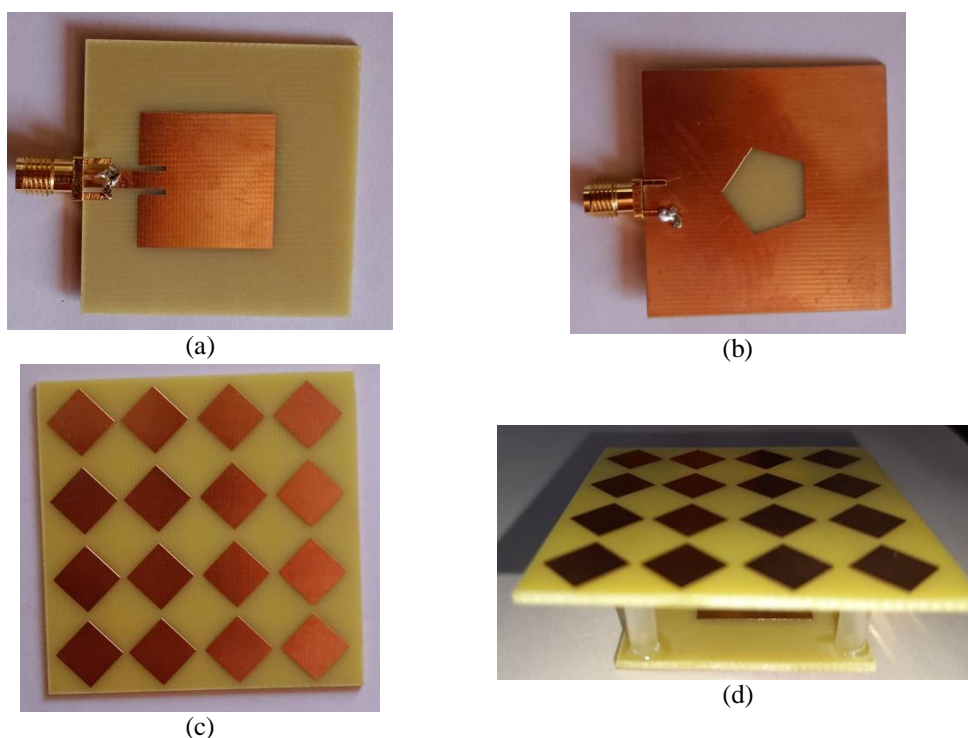


Fig. 11 Prototype of proposed antenna (a) Top View of radiator (b) Bottom view of radiator (c) Metasurface as LP to CP Converter (d) 3D view of proposed antenna

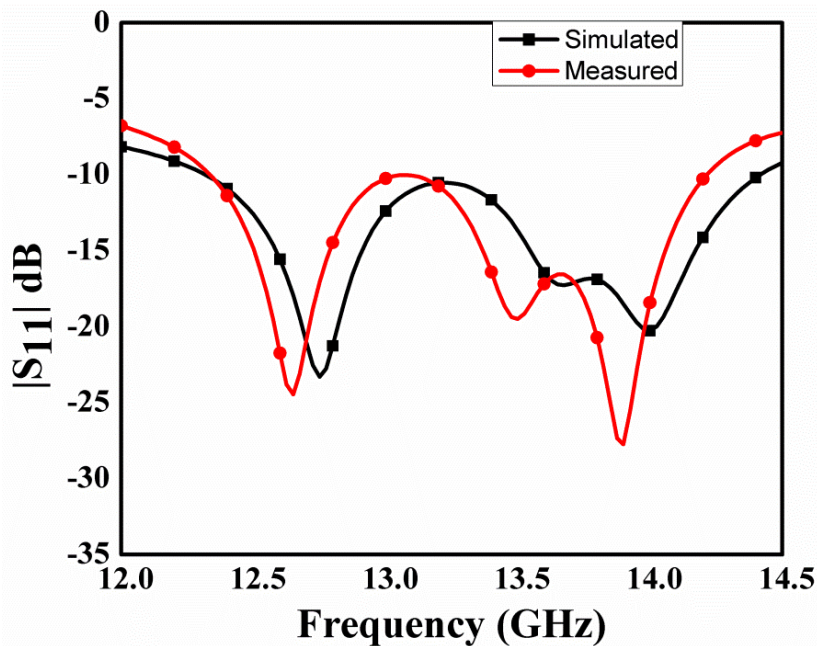


Fig. 12 Simulated and Measured |S₁₁| variation of proposed antenna

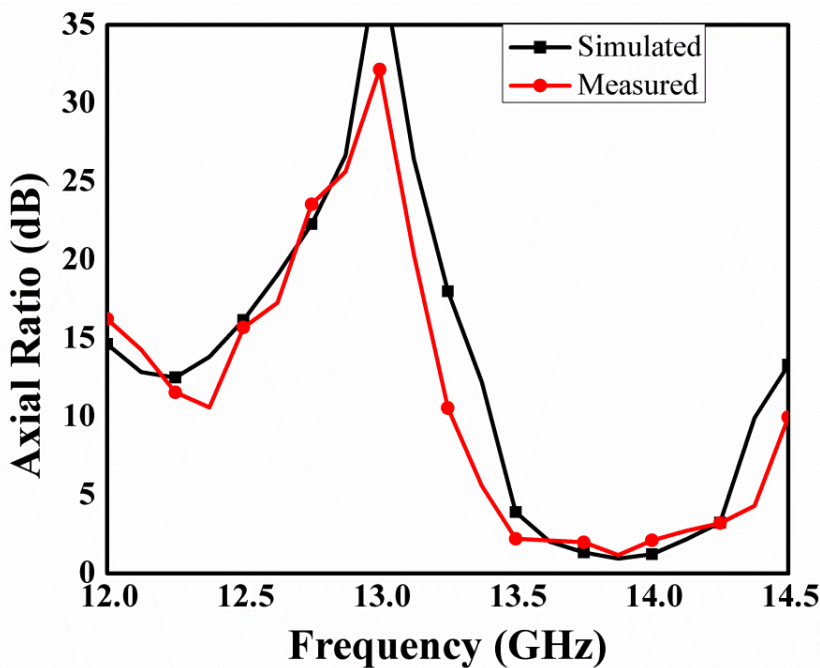
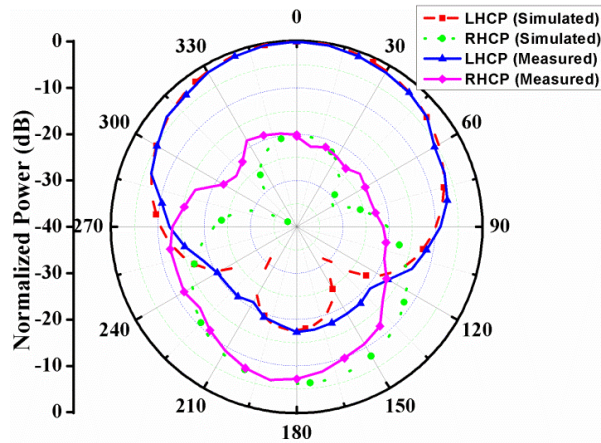
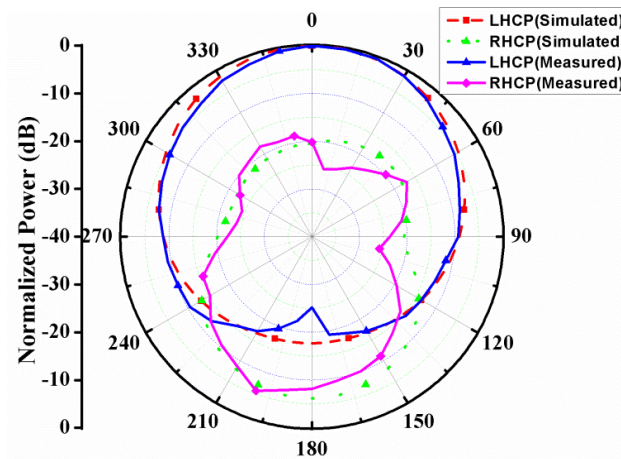


Fig. 13 Simulated and Measured axial ratio variation of proposed antenna

Fig. 14 shows the LHCP and RHCP radiation pattern of proposed antenna at 13.75 GHz in XZ and YZ plane. Two observations are obtained from Fig. 14: (a) the proposed antenna supports left handed circular polarization because LHCP is more dominant in comparison to RHCP (approx. 15 dB); (b) broadside radiation pattern is obtained in both XZ and YZ plane. Fig. 15 displays the gain (measured and simulated) and radiation efficiency (simulated) curve of proposed antenna. Gain is measured by using two antenna method [12]. There is good agreement between measured and simulated gain. Maximum gain in operating band is around 5.0 dBi. Radiation efficiency is also around 90% within the operating band. Table-2 lists the performance comparison of proposed antenna with other existing radiator in terms of antenna size, gain and bandwidth. After seeing the Table-2, it is confirmed that the proposed antenna provides better performance as compare to other existing antennas.



(a)



(b)

Fig. 14 LHCP and RHCP pattern of proposed antenna at 13.75 GHz (a) XZ plane (b) YZ plane

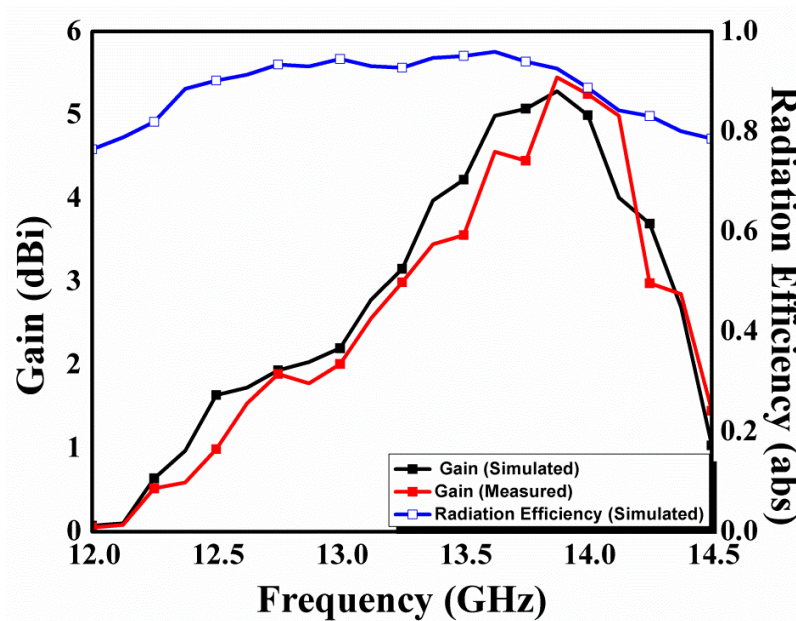


Fig. 15 Gain and Radiation Efficiency Curve of designed radiator

Table-2 Comparison of designed CP antenna with other existing antennas based on the concept of LP to CP converter

Antenna Design	Impedance Bandwidth (GHz)	Axial Ratio Bandwidth (GHz)	Antenna Size (mm ³)	Gain (dBi)
Microstrip Antenna [5]	0.05	0.05	120*120*1.6	5.0
Microstrip Antenna [6]	0.03	0.01	65.5*65*3.56	5.51
Slot Antenna [7]	2.0	0.6	60*60*3.0	5.5
Slot Antenna [8]	1.6	0.7	36*36*1.6	5.5
Proposed Antenna	2.1	0.75	40*40*1.6	5.5

V. CONCLUSION

This article explains the design of wideband printed antenna along with LP to CP converter. Rhombus shaped unit cell is arranged in periodic manner and suspended over the printed antenna for converting LP waves into circular waves from 13.5 GHz to 14.25 GHz. Inset feed improves the matching phenomenon of proposed radiator. Defected ground structure is used to reduce the quality factor of the radiator and improve the impedance bandwidth of the antenna. The proposed antenna operates from 12.34 GHz to 14.4 GHz. The designed antenna supports left handed circular polarization with broadside radiation characteristics. Good gain (around 5.0 dBi) value along with circular polarization features makes it suitable for Ku Band Satellite Applications.

REFERENCES

[1] Fu, S., Kong, Q., Fang, S., et al.: ‘Broadband circularly polarized microstrip antenna with coplanar parasitic ring slot patch for L-band satellite system application’, *IEEE Antennas Wirel. Propag. Lett.*, 2014, 13, pp. 943–946

[2] W.L. Stutzman and G.A. Thiele, “Antenna Theory and Design,” A John Wiley & Sons; (Hoboken, NJ); 2013

[3] X. Fang, K.W. Leung and E.H. Lim, “Singly-Fed dual-band circularly polarized dielectric resonator antenna”, *IEEE Antennas And Wireless Propagation Letters*, vol. 13, pp. 995-998, 2014

[4] C.W. Tong, H. Tang, W. Qin, W.W. Yang, X.F. Zhang and J.X. Chen, “Differentially inserted-fed compact dual-band circularly polarized dielectric resonator antenna,” *IEEE Antennas And Wireless Propagation Letters*, vol. 18, pp. 2498 – 2502, 2019

[5] H. L. Zhu, S. W. Cheung, Kwok Lun Chung, and T. I. Yuk, Member, “Linear-to-Circular Polarization Conversion Using Metasurface” *IEEE Transactions on Antennas and Propagation*, vol. 61, 4615-4623, 2013

[6] José Lucas da Silva Paiva, José Patrocínio da Silva, Antônio Luiz Pereira de Siqueira Campos and Humberto Dionísio de Andrade “Using metasurface structures as signal polarisers in microstrip antennas” *IET Microwaves, Antennas & Propagation*, vol. 13, 23-27, 2018

[7] Zi-Jian Hang, Wei Song and X Q Sheng, “Broadband Circularly Polarized Antenna by using polarization conversion metasurface” *ACES Journal*, 35, 656-661, 2020

[8] Jian Dong, Chang Ding and Jinjun Mo “A Low-Profile Wideband Linear-to-Circular Polarization Conversion Slot Antenna Using Metasurface” *Materials*, 13, 1-12, 2020

[9] M. Ramesh and YIP KB “Design Formula for Inset Fed Microstrip Patch Antenna” *Journal of Microwaves and Optoelectronics*, 3, 2003, 5-10

[10] Saininad Naik and Maria Pour, "A Miniaturized TM₂₁ Mode Circular Microstrip Patch Antenna," *Progress In Electromagnetics Research Letters*, Vol. 83, 45-50, 2019.

[11] Tanmoy Sarkar, A. Ghosh, L. L. K. Singh, Sudipta Chattopadhyay and Chow-Yen-Desmond Sim “DGS-Integrated Air-Loaded Wideband Microstrip Antenna for X- and Ku-Band” *IEEE Antennas and Wireless Propagation Letters*, vol. 19, 114-118, 2020

[12] C.A. Balanis, “Antenna Theory: Analysis and Design,” A John Wiley & Sons, INC., Publication, 3rd Edition, 2005.